



# A Radial Basis Function Collocation Method for Space-dependent Inverse Heat Problems

Muhammad Nawaz Khan<sup>1</sup>, Imtiaz Ahmad<sup>2</sup>, Hijaz Ahmad<sup>3</sup>

<sup>1</sup> Department of Basic Sciences, University of Engineering and Technology Peshawar 25000, Pakistan, Email: mnawaz77@gmail.com

<sup>2</sup> Department of Mathematics, University of Swabi 23430, Khyber Pakhtunkhwa, Pakistan, Email: imtiazkakakhil@gmail.com

<sup>3</sup> Department of Basic Sciences, University of Engineering and Technology Peshawar 25000, Pakistan, Email: hijaz555@gmail.com

Received March 20 2020; Revised April 20 2020; Accepted for publication April 29 2020.

Corresponding authors: H. Ahmad (hijaz555@gmail.com); I. Ahmad (imtiazkakakhil@gmail.com)

© 2020 Published by Shahid Chamran University of Ahvaz

**Abstract.** In this study, a radial basis function collocation method (RBF-CM) is proposed for the numerical treatment of inverse space-wise dependent heat source problems. Multiquadric radial basis function is applied for spatial discretization whereas for temporal discretization Runge-Kutta method of order four is employed. Numerical experiments for one, two and three-dimensional cases are included to test the efficiency and accuracy of the suggested method. Both non-rectangular and rectangular geometries with uniform and non-uniform points are taken into consideration and the obtained results are compared with the exact as well as with the techniques presented in recent literature.

**Keywords:** Meshless method, Radial basis function, Inverse heat source problem, Non-uniform nodes, Non-rectangular domains.

## 1. Introduction

The inverse heat conduction problems (IHCP) with unknown space dependent heat source are mostly highlighted in the conduction, transportation, hydrology, and diffusion process in natural materials. Mathematically the inverse heat conduction problem with unknown space dependent heat source is defined as

$$w_t = \Delta w(x,t) + f(x), \quad x \in \Omega \subset \mathbb{R}^n, \quad t > 0, \quad (1)$$

where  $\Delta$  is the Laplace operator,  $w(x,t)$  is the state variable and  $f(x)$  is the physical source term, which is the unknown space dependent heat source. Sad to say that the characteristics of  $w(x,t)$  and the sources term in actual problems are always unknown to the nature of these types of IHCP are known as ill-posed problems [1-3]. Generally, the recovery of heat source term with complete accuracy is impossible under the restricted boundary conditions. Such types of problems are unstable caused by or ascribable to the obtaining of unknown variables from the direct observations which contain some measurement errors. The construction of an accurate and stable numerical method is very difficult due to the ill-posedness and ill-conditioning of the discretized matrix.

A verity of numerical techniques is used to investigate IHCP such as the iterative regularization technique [4], boundary element method [5], radial basis functions (RBFs) based method [6], method of fundamental solution (MFS) [7,8], Lie-group method (LGM) [9], meshless collocation procedures [10] and Haar wavelet collocation multi-resolution method [3].

As most practical problems in applied sciences and engineering are not limited to low dimensions but modeled in higher dimensions. Thus dealing such problems bring a lot of computational cost in terms of mesh generations using mesh-based methods, like finite difference method (FDM) [11], variation iteration method (VIM) [12], finite volume method (FVM) [13], variation iteration algorithms [14-17] and other numerical/analytical methods [18-20]. This computational cost is low in one dimension but increase as dimension increases. Moreover, complex or irregular problem geometries cannot be handled easily when moving discontinuities occur, such as propagation of cracks and flames. In such a case re-meshing and re-alignment of meshes are needed which itself is a tedious job. Thus RBFs methods become a viable option in such a scenario. As the only geometric property needed in RBFs approximation is their pairwise distance between data points. This can be done easily regardless of the problem geometry and dimension. Moreover, no prior mesh connectivity information is needed amongst the data points.

Recently, the meshless methods got practical importance and broadly attention for the solution of different kind of partial differential equations (PDEs) arises in almost all disciplines of engineering. They do not require any prior information about mesh connectivity and have no sensitivity to mesh alignment. Other features are their achievement of spectral accuracy, low computational cost and their flexibility to complex shape domains. While in these procedures, the problem domain is represented by a set of scattered data nodes provided in the form of initial data.

From the above mentioned characteristics, these methods distinguishable from FEM, FDM and FVMs and brings more



flexibility in applications perspective to problems of engineering and physical sciences. These methods became popular amongst the scientific community and now are a rich area of research need to be explored. In many computational challenging problems, the meshless methods delivered well and showed promising performance [21-23].

### 1.1 Formulation of the inverse heat source Problem

Considering one-dimensional IHCP

$$\frac{\partial w(x,t)}{\partial t} = \frac{\partial^2 w(x,t)}{\partial x^2} + f(x), \quad (x,t) \in ((a,b),(0,T)), \quad (2)$$

with the following conditions

$$w(x,0) = \varphi(x), \quad a \leq x \leq b, \quad (3)$$

$$w(a,t) = g_1(t), \quad w(b,t) = g_2(t), \quad 0 \leq t \leq T, \quad (4)$$

$$w(x,T) = \eta(x), \quad a \leq x \leq b, \quad (5)$$

where the functions  $\varphi$ ,  $g_1$ ,  $g_2$  and  $\eta$  are known and  $T$  is the final time, whereas  $w$  and  $f$  are unknown functions to be calculated.

## 2. Global Meshless Scheme

A real-valued function is called radial basis function if defined on norms of the input set of data points with the independent variable  $x$ , i.e.,  $\Psi(x, x_i, c) = \psi(\|x - x_i\|, c)$ , where  $x_i = 1, 2, \dots, N$ . The shape of these radial basis functions which are one parameter curves is dependent on an unknown parameter which is called shape parameter  $c$ . In the current study, we utilize multiquadric RBF  $\psi(x) = \sqrt{r^2 + c^2}$ , where  $r = \|x - x_i\|$ . We choose  $N$  nodes  $(x_i, i = 1, 2, \dots, N)$  in the domain. The approximate function  $w(x,t)$  is presented by  $w^N(x)$ . The RBF approximation is of the form

$$w^N(x) = \sum_{i=1}^N \lambda_i \psi_i = \Psi^T(x) \Lambda \quad (6)$$

where  $\Psi(x) = [\psi_1(x), \psi_2(x), \dots, \psi_N(x)]^T$ ,  $\Lambda = [\lambda_1, \lambda_2, \dots, \lambda_N]^T$ .

Let us suppose  $w^N(x_i) = w_i$ , then

$$A \Lambda = W \quad (7)$$

where  $W = [w_1, w_2, \dots, w_N]^T$

$$A = \begin{bmatrix} \Psi^T(x_1) \\ \Psi^T(x_2) \\ \dots \\ \Psi^T(x_N) \end{bmatrix} = \begin{bmatrix} \psi_1(x_1) & \psi_2(x_1) & \dots & \psi_N(x_1) \\ \psi_1(x_2) & \psi_2(x_2) & \dots & \psi_N(x_2) \\ \vdots & \vdots & \ddots & \vdots \\ \psi_1(x_N) & \psi_2(x_N) & \dots & \psi_N(x_N) \end{bmatrix}$$

It follows from equation (6) and (7) that

$$w^N(x) = \Psi^T(x) A^{-1} W = \mathbb{N}(x) W \quad (8)$$

where  $\mathbb{N}(x) = \Psi^T(x) A^{-1}$ .

Here, we suppose a transformation  $u(x,t) = w_t(x,t)$ . Hence, from equations (2)-(5), we get

$$\frac{\partial u(x,t)}{\partial t} = \frac{\partial^2 u(x,t)}{\partial x^2}, \quad (9)$$

$$u(x,0) = \dot{\varphi}(x) = 0, \quad (10)$$

$$u(a,t) = \dot{g}_1(x), \quad u(b,t) = \dot{g}_2(x).$$

By applying the RBFCM to equation (9), we get

$$\frac{du_i}{dt} = \mathbb{N}_{xx}(x_i) u, \quad i=1,2,\dots,N \quad (11a)$$



where

$$\begin{aligned}
 N_{xx}(x_i) &= [N_{1xx}(x_i), N_{2xx}(x_i), \dots, N_{Nxx}(x_i)], \\
 N_{jxx}(x_i) &= \frac{\partial^2 N_j(x_i)}{\partial x^2}, \quad j = 1, 2, \dots, N.
 \end{aligned}
 \tag{11b}$$

Writing this system in vector form as

$$\frac{dU}{dt} = Z_{xx}U,
 \tag{12}$$

The corresponding initial and boundary conditions are

$$U(t_0) = \begin{bmatrix} 0 \\ u(x_1) \\ u(x_2) \\ \dots \\ u(x_N) \end{bmatrix}
 \tag{13}$$

$$u_1(t) = \dot{g}_1(t), \quad u_N(t) = \dot{g}_2(t),
 \tag{14}$$

To solve the system of ordinary differential equations (12)-(14), we use the following classical four order Runge-Kutta Scheme to get the numerical solution of  $u(x,t)$  as follows

$$\begin{aligned}
 U^{n+1} &= U^n + \frac{\Delta t(K_1 + 2K_2 + 2K_3 + K_4)}{6}, \\
 K_1 &= F(U^n), \quad K_2 = F\left(U^n + \frac{\Delta t}{2}K_1\right), \\
 K_3 &= F\left(U^n + \frac{\Delta t}{2}K_2\right), \quad K_4 = F(U^n + \Delta tK_3).
 \end{aligned}
 \tag{15}$$

Integrating  $u(x,t) = w_t(x,t)$  with respect to  $t$  from  $t_0$  to  $t$ , the  $w(x,t)$  can be attained. The source term  $f(x,t)$ , which is unknown can be obtained from equation (2) directly, as

$$f(x) = \frac{\partial w(x,t)}{\partial t} \Big|_{t=T} - \frac{\partial^2 w(x,T)}{\partial x^2}
 \tag{16}$$

$$f(x) = u(x,T) - \varphi''(x)
 \tag{17}$$

### 3. Numerical Results and Discussion

To implement the LRBFD in the one-dimensional case, we introduce noisy data on the boundary, which is defined as

$$\hat{w}_b = w_b \times (1 + e \times rand),
 \tag{18}$$

where  $rand$  denotes the random number,  $\hat{w}_b$  is the noise data on the accessible boundary,  $e$  is the noise level, which is expressed as  $e = s / 100$  and  $s$  is the percentage of noise. For verification purpose one dimensional (1D), two dimensional (2D) and three dimensional (3D) inverse source heat problems for high noise data as well as on both regular as well as irregular domains are considered and different error norms like the absolute ( $L_{abs}$ ), relative root mean square (RES) and root mean square (RMS) are obtained for comparison purposes and applicability of the purposed method. The error norms which will be considered are defined as

$$\begin{aligned}
 L_{abs}(f) &= |f_{Ex(i)} - f_{Nu(i)}|, \quad i = 1, 2, \dots, N \\
 RMS(f) &= \sqrt{\frac{1}{N} \sum_{i=1}^N (L_{abs}(f))^2}, \\
 RES &= \sqrt{\frac{\sum_{i=1}^N (L_{abs}(f))^2}{\sum_{i=1}^N (f_{Nu(i)})^2}},
 \end{aligned}
 \tag{19}$$

where  $f_{Nu}$  and  $f_{Ex}$  represents numerical and exact values respectively. For  $w$  the error norms  $L_{abs}$ , RMS and RES are calculated in a similar way.

**Test Problem 1.** Considering one-dimensional case with the beneath exact solution  $w(x,t)$  and heat source  $f(x)$

$$w(x,t) = \sin(2\pi x) + x^2 + 2tx, \quad f(x) = 4\pi^2 \sin(2\pi x) + 2x - 2.
 \tag{20}$$

In Table 1 the error norms  $RMS(f)$  and  $RES(f)$  of the RBFCM in the computational domain  $[0,1]$  are compared with the method given in [8]. In Fig. 1 we have shown the comparison of exact and numerical solutions of  $w(x,t)$  and  $f(x)$  whereas Figure 2 shows numerical results of heat source function for various noise levels, these results show that the RBFCM can handle this problem accurately even for a high noise level up to  $s = 10\%$ .



**Table 1.** Numerical results at  $s = 0.1\%$ ,  $c = 10$  and  $N = 51$  for Test Problem 1.

t	RMS(f)	RMS(f)	RMS(f)	RMS(f)
	RBFCM	MFS [8]	RBFCM	MFS [8]
1.5	$9.8792 \times 10^{-4}$	$6.134 \times 10^{-2}$	$1.3834 \times 10^{-4}$	$2.279 \times 10^{-3}$
3	$6.2879 \times 10^{-4}$	$5.181 \times 10^{-3}$	$8.8048 \times 10^{-5}$	$1.811 \times 10^{-4}$
5	$7.4759 \times 10^{-5}$	$3.562 \times 10^{-3}$	$1.0468 \times 10^{-5}$	$1.290 \times 10^{-4}$
7	$2.4000 \times 10^{-3}$	$7.080 \times 10^{-4}$	$3.3914 \times 10^{-4}$	$2.574 \times 10^{-5}$
10	$1.1800 \times 10^{-2}$	$1.401 \times 10^{-3}$	$1.7000 \times 10^{-3}$	$5.079 \times 10^{-5}$

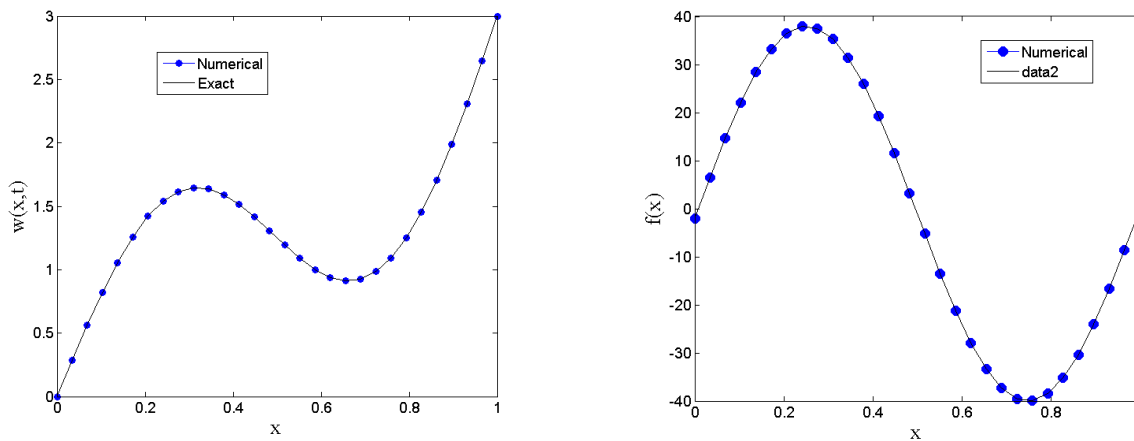


**Fig. 1.** Numerical solution of  $w(x,t)$  and  $f(x)$  using exact data using  $c = 7$ ,  $N = 30$  and  $t = 1$  for Test Problem 1.

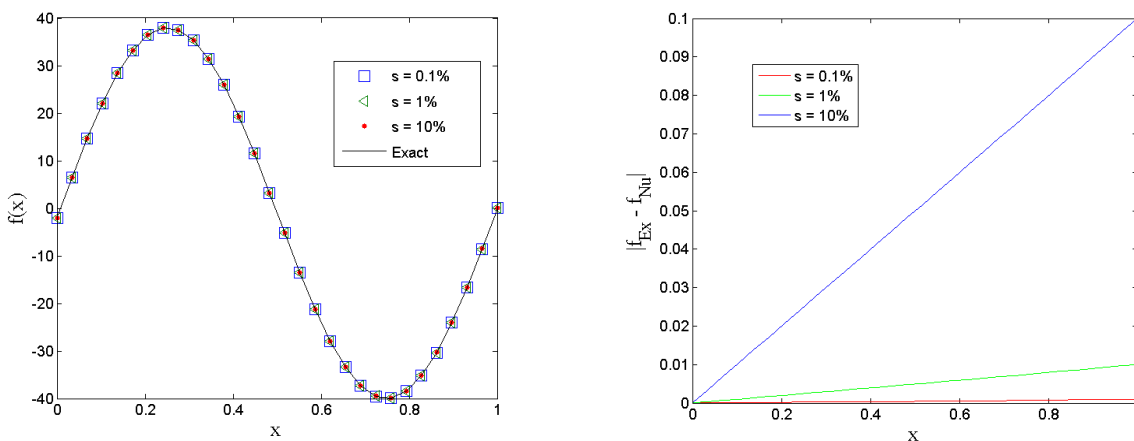


**Fig. 2.** Numerical results for different noise levels using  $c = 7$ ,  $N = 30$  and  $t = 1$  for Test Problem 1.

**Test Problem 2.** Again considering the one-dimensional case with the following exact solution and heat source

$$w(x,t) = -(e^{-\pi^2 t} - 2)\sin(\pi x), \quad f(x) = 2\pi^2 \sin(\pi x). \tag{21}$$

Numerical results obtained by the RBFCM are shown in Figure 3 using various noise levels and these results have been compared with Tikhonov regularization boundary element method (TRBEM) [5], Boundary element method (BEM) [4], Lie-group adaptive method (LGAM) [9], Lie-group numerical differential method (LGNDM) [9] and method of fundamental solutions (MFS) [7]. It can be observed from the figure that the RBFCM can handle this challenging problem with considerable good accuracy. It is also noted that in all the methods  $N > 32$  is taken but the RBFCM gives better results even at  $N = 20$ . This problem has been considered in [5] as the most challenging case to capture the heat source accurately due to its ill-posedness. From the error profiles, one can see that the results are accurate and well satisfactory, even with the noise level up to  $s = 10\%$  as shown in Figure 2.

**Test Problem 3.** Considering two-dimensional case [1] in which exact solution

$$w(x,y,t) = (\cos(2x) + \cos(2y))(1 - e^{-4t}), \tag{22}$$

and exact source term

$$f(x,y) = 4(\cos(2x) + \cos(2y)). \tag{23}$$

Fig. 5 shows the error for heat source utilizing exact data for the Least-squares method (LSM) and Tikhonov regularization method (TRM) [1] and the RBFCM whereas for noise data ( $s = 1\%$  and  $s = 2\%$ ) the results are shown in Fig. 6. From these figures, it is cleared that the accuracy of the RBFCM is more accurate than the methods given in [1] for both exact and noise data.



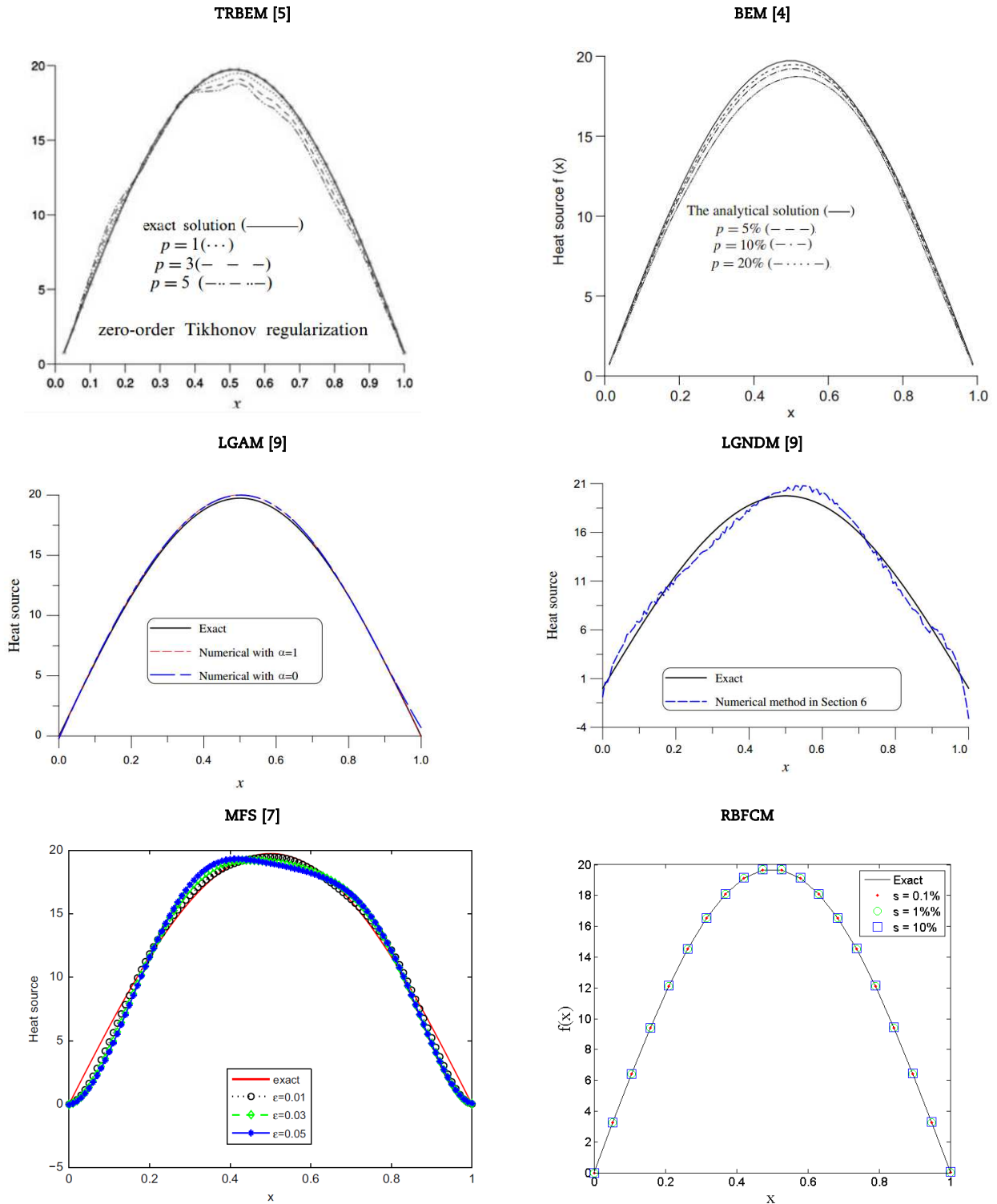


**Fig. 3.** Comparison of different methods (TRBEM [5], BEM [4], LGAM [9], LGNDM [9], MFS [7]) with the RBFCM using  $c=8$  and  $N=20$  for Test Problem 2.

**Test Problem 4.** Considering two-dimensional case [7] in which exact solution

$$w(x,y,t) = e^{x-t} \cos(\sqrt{2}y) - x^3 - y^3, \tag{24}$$

and exact source term

$$f(x,y) = 6x + 6y. \tag{25}$$

In Fig. 7 different types of non-rectangular domains are shown whereas Fig. 8 shows the comparison of the proposed method with MFS [7] on domain 1, which shows that the accuracy of the RBFCM is more accurate than the method given in [7]. In Fig. 9 the error on domain 1 for the heat source  $f(x,y)$  is shown for  $s = 0.1\%$ ,  $10\%$ . The error on domain 2 for exact data and  $s = 10\%$  is shown in Fig. 10. The heat source  $f(x,y)$  is shown in Fig. 11 on domain 3. Figs. 12 - 13 show that the suggested method gives more accurate results on domain 3 using uniform points as well as Halton points.



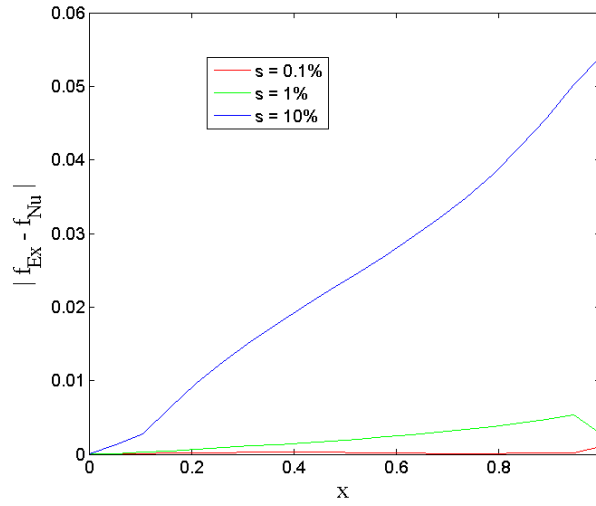


Fig. 4. Error Comparison of  $f(x)$  at different noise levels using  $c = 8$ ,  $N = 20$  and  $t = 1$  for Test Problem 2.

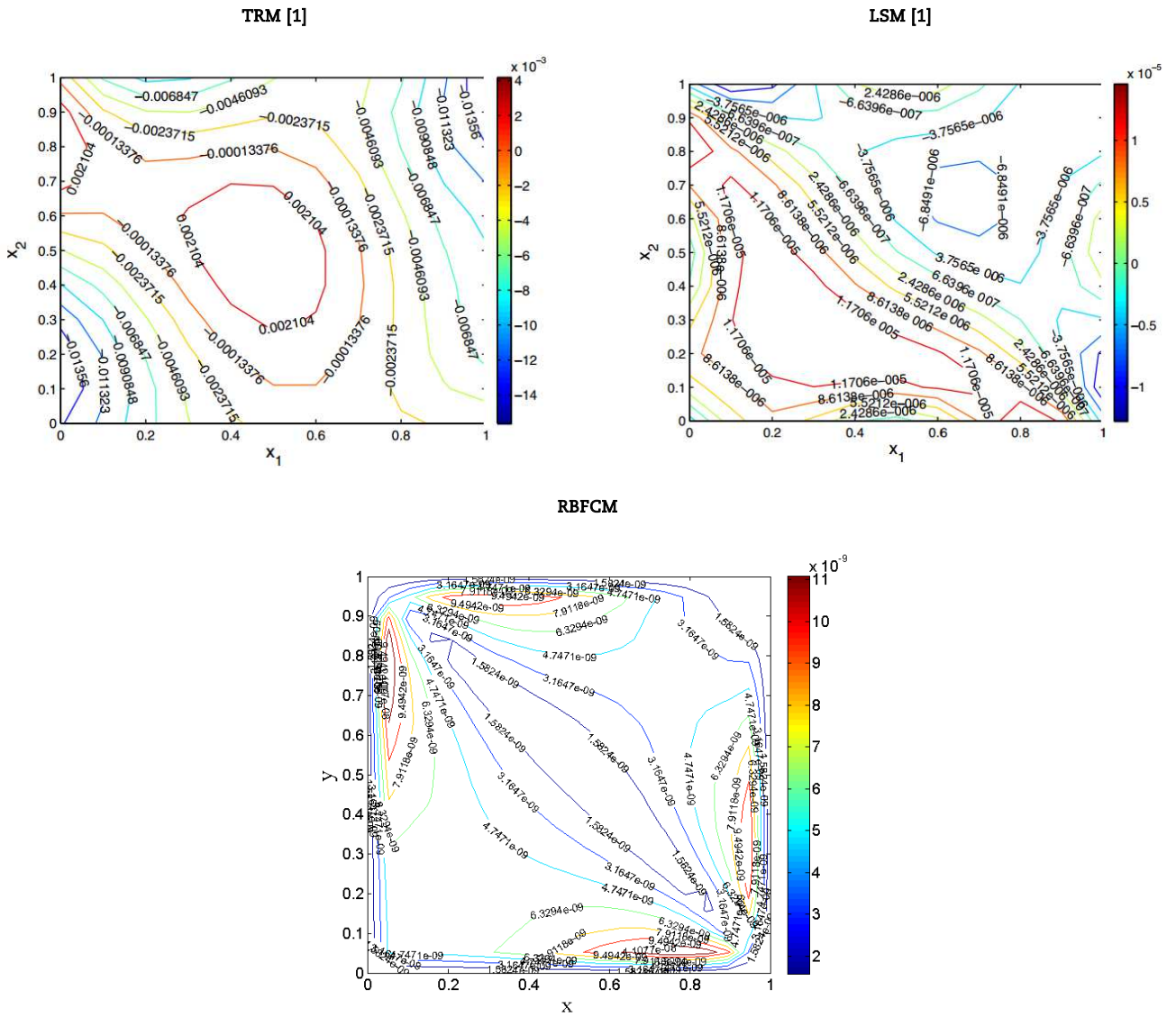
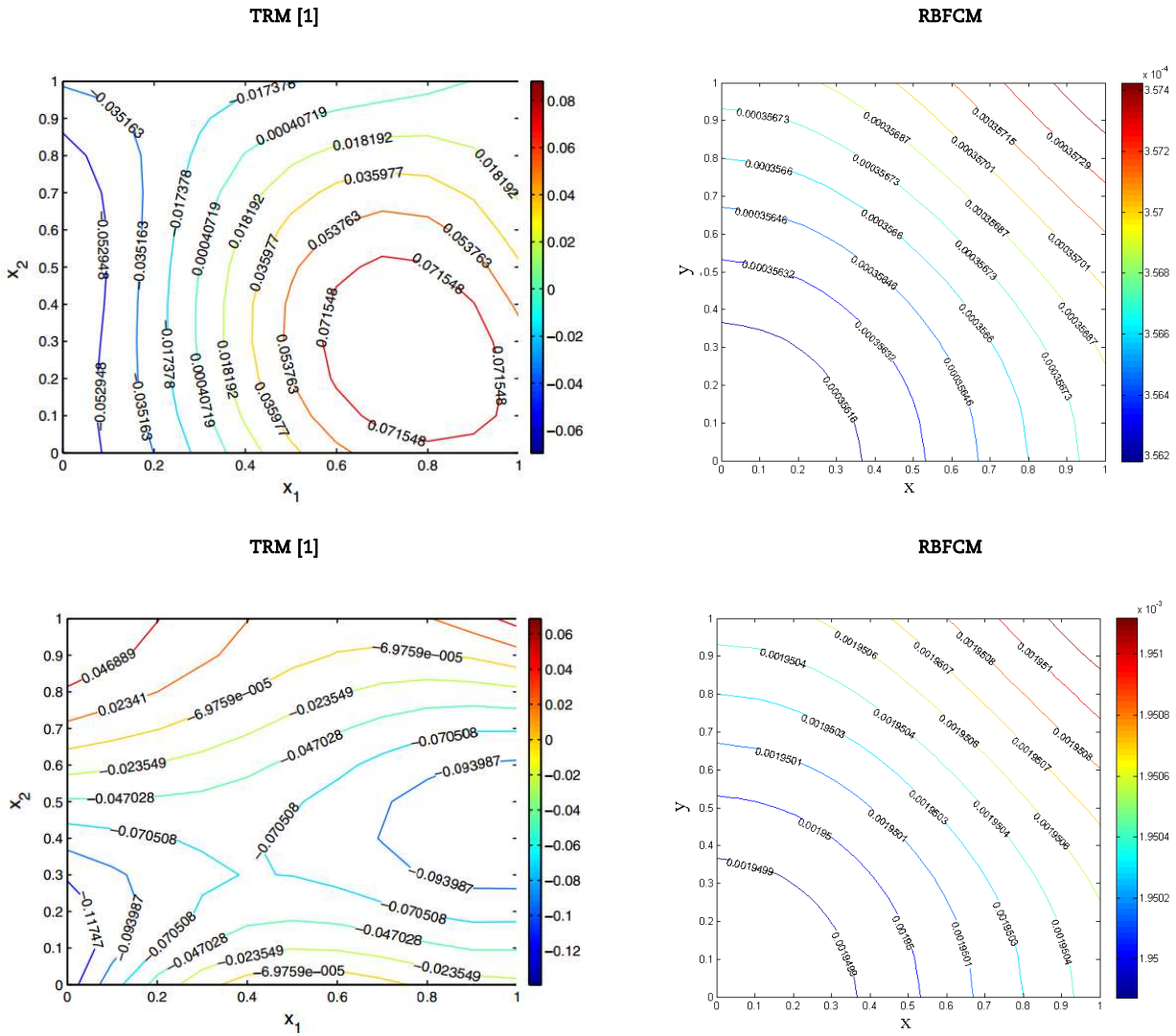
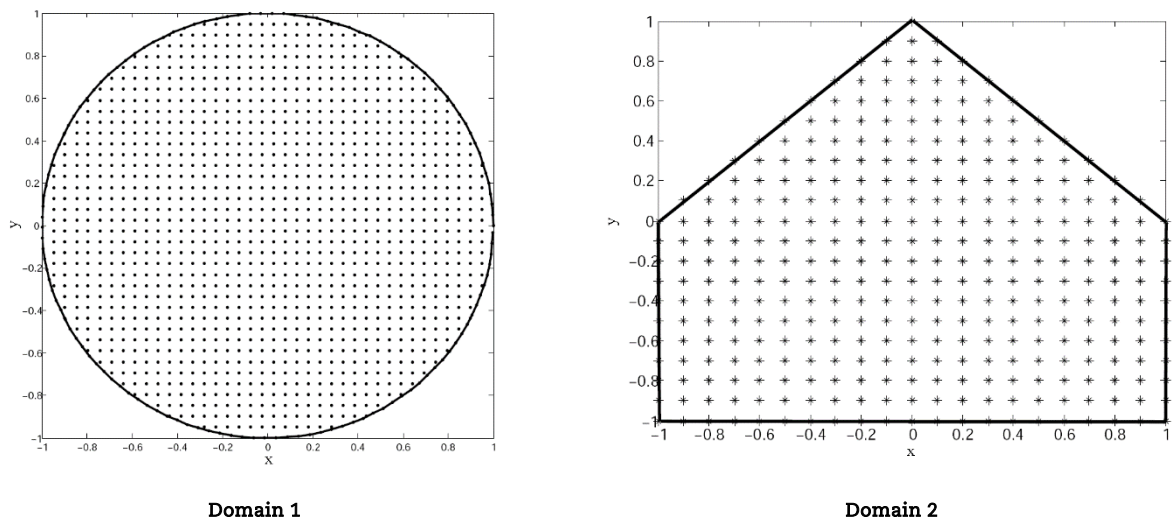


Figure 5. Error comparison for  $f(x,y)$  of the proposed method with the methods given in [1] using exact data at  $c = 0.3$  and  $N = 225$  for Test Problem 3.



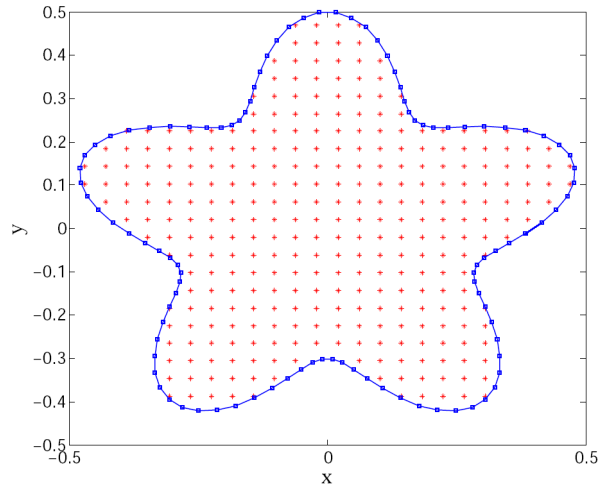


**Fig. 6.** Error comparison for  $f(x,y)$  of the proposed method with the methods given in [1] at noise data  $s = 1\%$  (1st row) and  $s = 2\%$  (2nd row) using  $c = 0.3$  and  $N = 225$  for Test Problem 3.



**Fig. 7.** The configuration of non-rectangular domains.





Domain 3

Fig. 7. The configuration of non-rectangular domains.

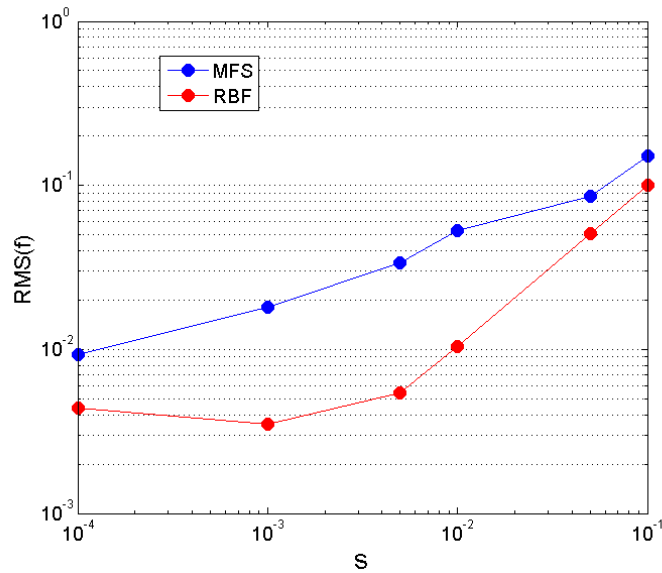


Fig. 8. Numerical results at various amounts of noise using  $c = 0.2$  and  $N = 400$  for Test Problem 4.

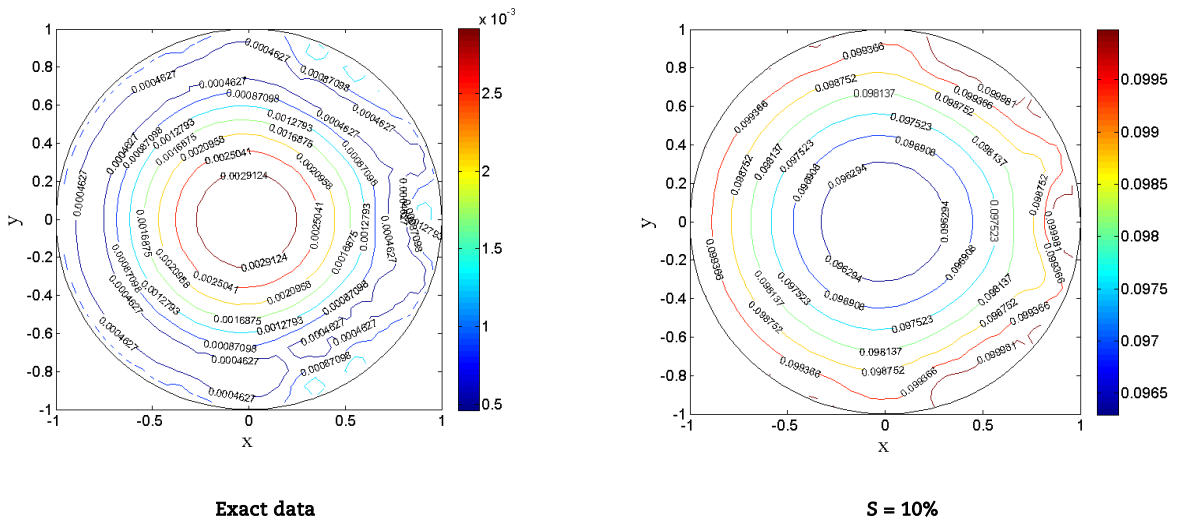


Fig. 9. The Labs error norm of  $f(x,y)$  on domain 1 using  $c = 0.2$  and  $N = 402$  for Test Problem 4.



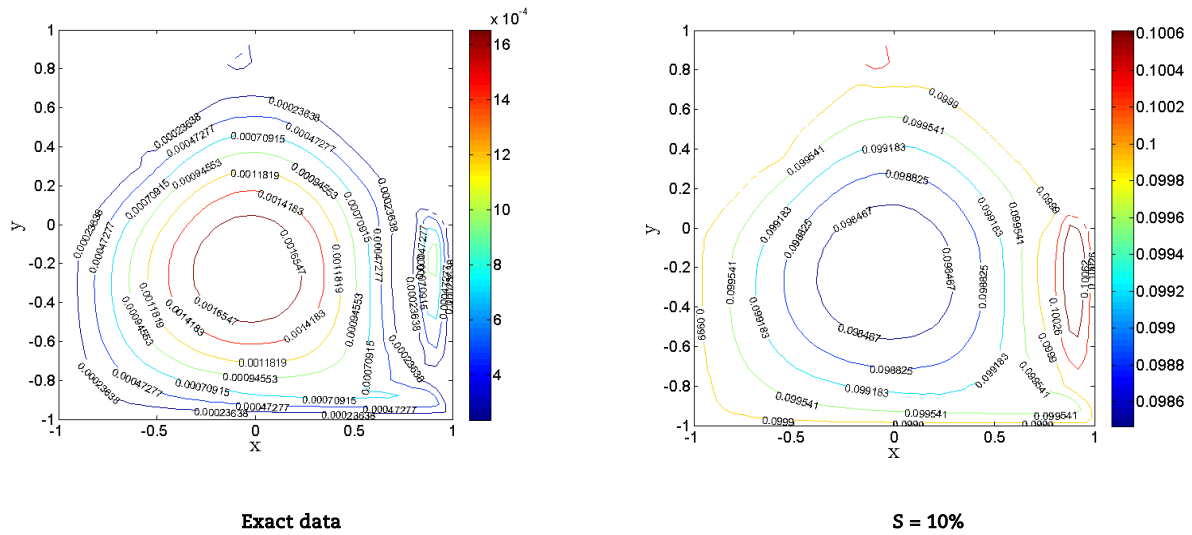


Fig. 10. The Labs error norm of  $f(x,y)$  on domain 2 using  $c = 0.2$  and  $N = 331$  for Test Problem 4.

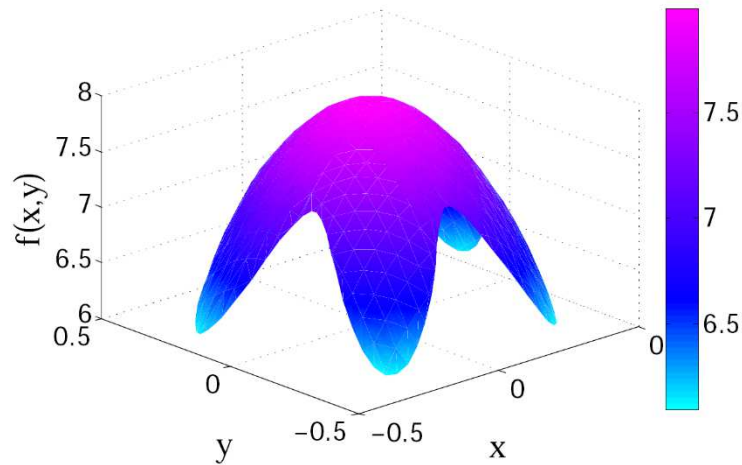


Fig. 11. Numerical results of heat source  $f(x,y)$  on domain 3 using exact data at  $c = 0.068$  and  $N = 150$  for Test Problem 4.

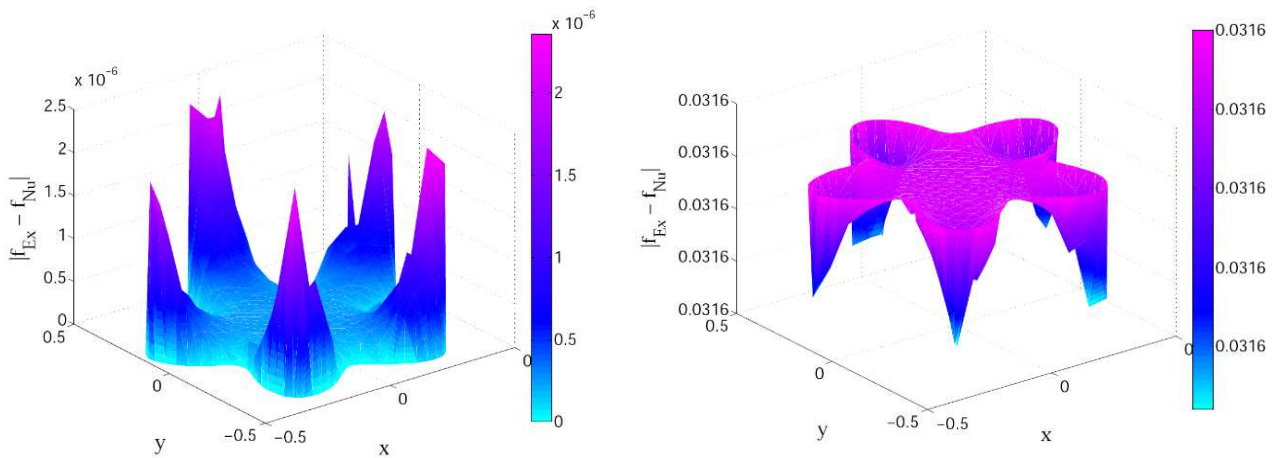


Fig. 12. The Labs error norm of  $f(x,y)$  on domain 3 with uniform points using exact data (left) and  $s = 5\%$  (right) at  $c = 0.068$  and  $N = 150$  for Test Problem 4.



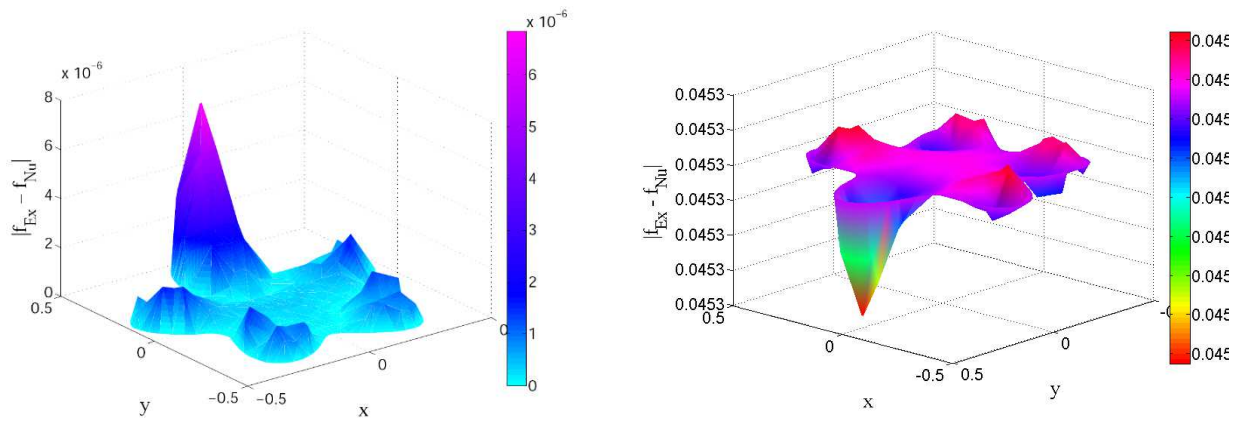


Fig. 13. The Labs error norm of  $f(x,y)$  on domain 3 with Halton points using exact data (left) and  $s = 5\%$  (right) at  $c = 0.09$  and  $N = 150$  for Test Problem 4.

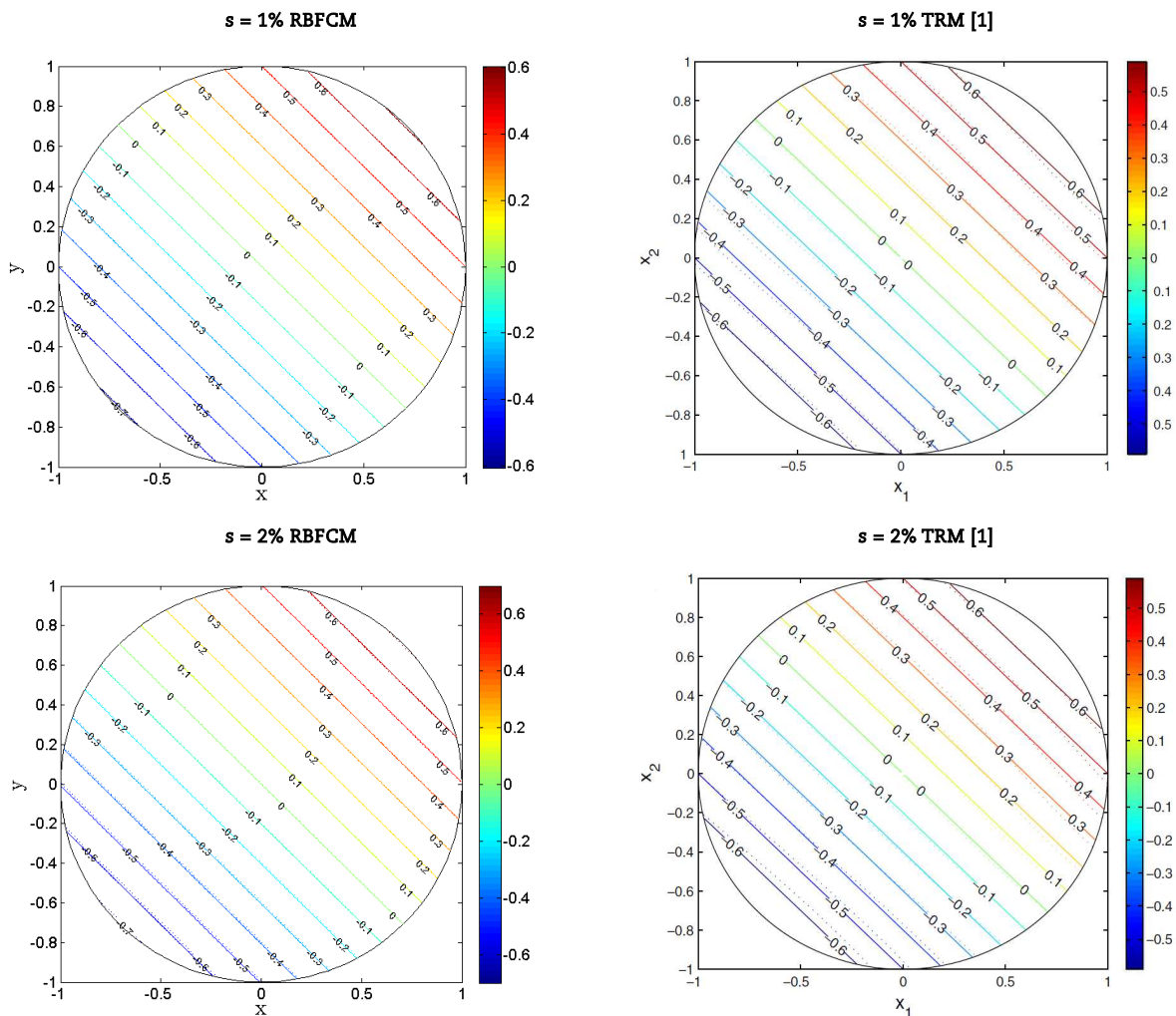


Fig. 14. Comparison of exact (–) and numerical (...) heat source at various noise levels using  $c = 0.2$  and  $N = 402$  for Test Problem 5.

**Test Problem 5.** Considering the two-dimensional IHCP [1] with the exact solution

$$w(x,y,t) = (x+y)\frac{t}{2}, \tag{26}$$

and exact source term

$$f(x,y) = \frac{1}{2}(x+y). \tag{27}$$

Fig. 14 shows the results of heat source obtained employing the RBFCM for noise data and  $s = 1\%$   $s = 2\%$ . In this figure, we have compared our results with exact as well as with the results given in [1]. One can observe that the RBFCM produced bettered results as compared to the results given in [1].



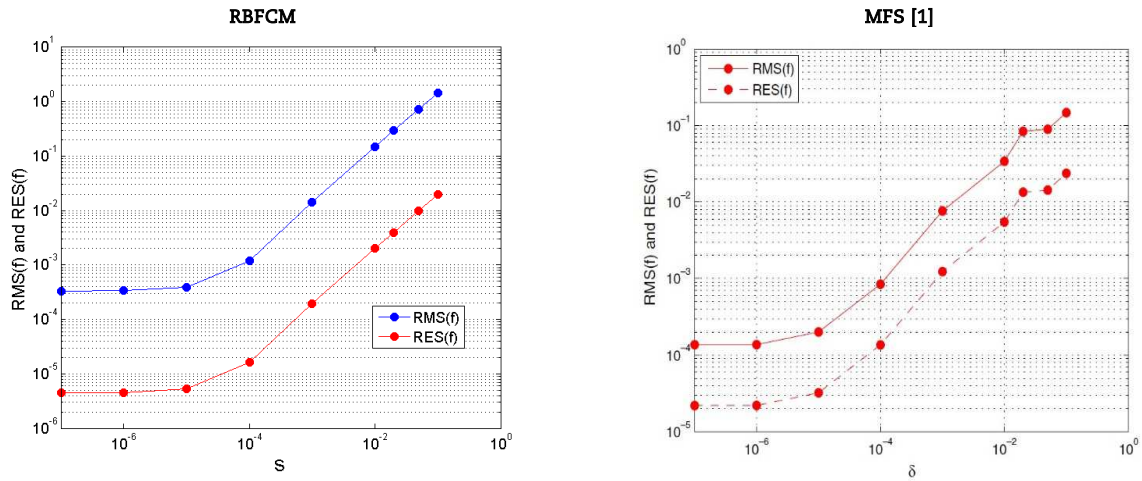


Fig. 15. The RBFCM versus the MFS [1] using  $c = 0.9$  and  $N = 125$  for Test Problem 6.

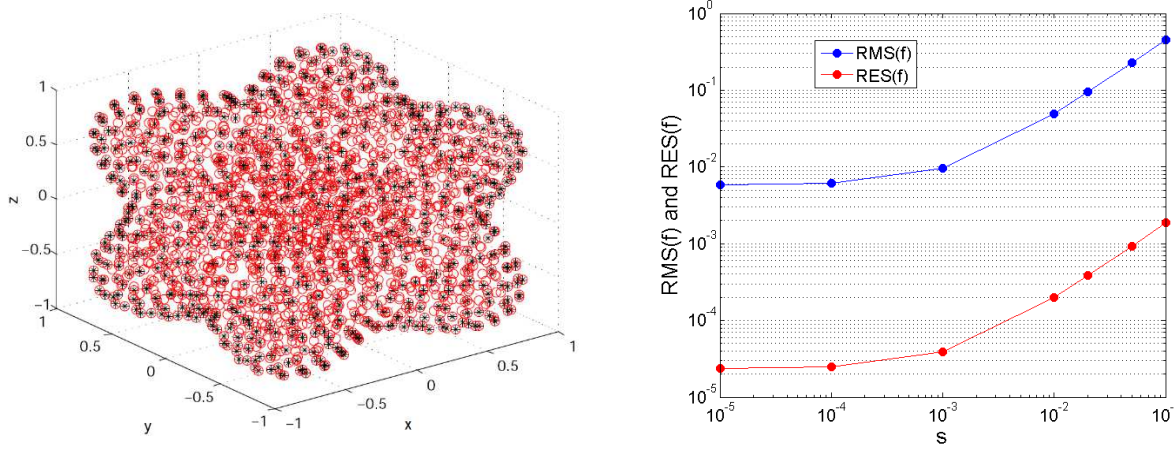


Fig. 16. Computational domain (left) and numerical results (right) using  $c = 0.3$  and  $N = 2046$  for Test Problem 6.

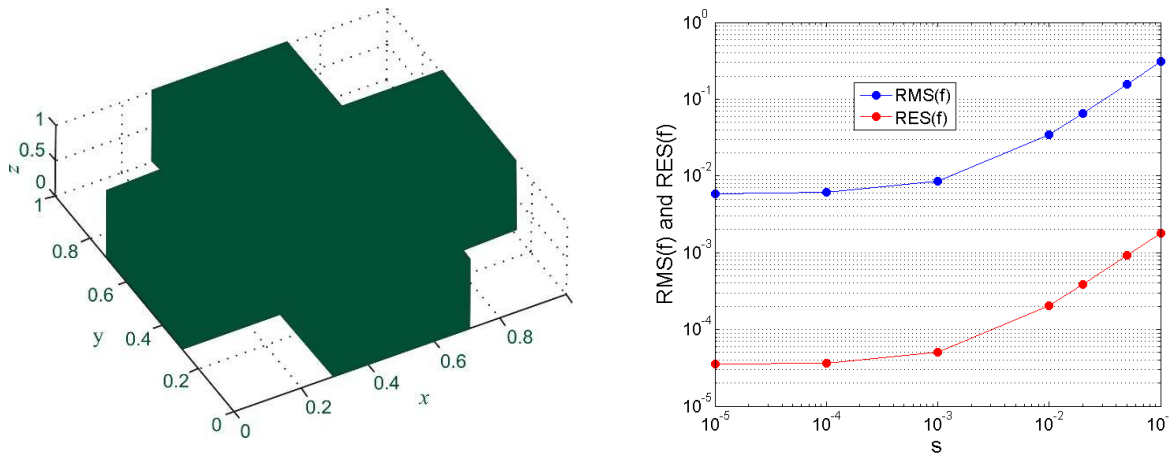


Fig. 17. Computational domain (left) and numerical results (right) using  $c = 0.02$  and  $N = 935$  for Test Problem 6.

**Test Problem 6.** Considering the three-dimensional case [1] in which the exact solution is

$$w(x,y,z,t) = (\cos(2x) + \cos(2y) + \cos(2z))(1 - e^{-4t}), \quad 1 \leq t \leq 2, \tag{28}$$

and exact source term

$$f(x,y,z) = 4(\cos(2x) + \cos(2y) + \cos(2z)). \tag{29}$$

In Fig. 15 the results obtained of the suggested technique the RBFCM for Test Problem 6 are compared with the results given [1]. It can be perceived from the figure that the RBFCM produced better results in this case as well. In Figs. 16-17 again validates stable computations and efficiency of the RBFCM, and show that the proposed method produces better results in irregular domains.



## 4. Conclusion

In this study, we have mainly focused on the applicability and performance of the radial basis function collocation method to a class of space-wise dependent heat source problems. The numerical results of the method are comparatively accurate and efficient than the existing techniques in recent literature and we have observed high accuracy, effectiveness, robustness and less computational cost by conducting various numerical experiments. For verification purpose 1D, 2D and 3D inverse source heat problems for high noise data by considering both regular as well as irregular domains excellent accurate solutions have been obtained. To better understand the physical phenomena of these models, we have also used numerical simulation technology to give some graphics of the results obtained, which revealed that the RBFCM is reliable to solve the space-wise dependent heat source problem. The discussion of the results and graphically illustrated solutions revealed that our proposed approach is an efficient and reliable tool for the solution of inverse problems.

## Acknowledgments

The authors wish to acknowledge the anonymous referees whose suggestions have helped to improve the quality of our paper.

## Conflict of Interest

The authors declared no potential conflicts of interest with respect to the research, authorship and publication of this article.

## Funding

The authors received no financial support for the research, authorship and publication of this article.

## References

- [1] Liang Y, Lian Y. F., Li F. C., A meshless method for solving an inverse spacewise-dependent heat source problem, *Journal of Computational Physics* 228 (1) (2009) 123-136.
- [2] Rou C., Whitney Y., Yousheng X., Luoding Z., Scalings of inverse energy transfer and energy decay in 3-d decaying isotropic turbulence with non-rotating or rotating frame of reference, *Journal of Applied and Computational Mechanics* 5 (4) (2019) 639-646.
- [3] Srivastava MH, Ahmad H, Ahmad I, Thounthong P, Khan NM., Numerical simulation of three-dimensional fractional-order convection-diffusion PDEs by a local meshless method, *Thermal Science*, 2020, DOI: 10.2298/TSCI200225210S.
- [4] Tomas J., Daniel L., Determination of a spacewise dependent heat source, *Journal of Computational and Applied Mathematics* 209 (1) (2007) 66-80.
- [5] Adrian F., Daniel L., The boundary-element method for the determination of a heat source dependent on one variable, *Journal of Engineering Mathematics* 54 (4) (2006) 375-388.
- [6] Shidfar A., Darooghehgomofrad Z., A numerical algorithm based on RBFs for solving an inverse source problem, *Bulletin of the Malaysian Mathematical Sciences Society* 40 (2017) 1149-1158.
- [7] Wei T., Wang J., Simultaneous determination for a space-dependent heat source and the initial data by the MFS, *Engineering Analysis with Boundary Elements* 36 (12) (2012) 1848-1855.
- [8] Ahmadabadi M. N., Ameri M. A., Ghaini F. M., The method of fundamental solutions for the inverse space-dependent heat source problem, *Engineering Analysis with Boundary Elements* 33 (10) (2009) 1231-1235.
- [9] Liu C.-S., An iterative algorithm for identifying heat source by using a DQ and a Lie-group method, *Inverse Problems in Science and Engineering* 23 (1) (2015) 67-92.
- [10] Siraj-ul-Islam, Ismail S., Meshless collocation procedures for time-dependent inverse heat problems, *International Journal of Heat and Mass Transfer* 113 (2017) 1152-1167.
- [11] Niasar M. B., Ameri M. A., Moving mesh non-standard finite difference method for non-linear heat transfer in a thin finite rod, *Journal of Applied and Computational Mechanics* 4 (3) (2018) 161-166.
- [12] Ahmad, H., Khan, T. A., Yao, S.-W., Numerical solution of second order Painlevé differential equation, *Journal of Mathematics and Computer Science* 21 (2) (2020) 150-157.
- [13] Flegg J. A., Byrne H. M., Flegg M. B., McElwain D. S., Wound healing angiogenesis: the clinical implications of a simple mathematical model, *Journal of Theoretical Biology* 300 (2012) 309-316.
- [14] Ahmad, H., Khan, T. A., Variational iteration algorithm I with an auxiliary parameter for the solution of differential equations of motion for simple and damped mass-spring systems, *Noise & Vibration Worldwide* 51 (2020) 12-20.
- [15] Ahmad, H., Seadawy, A. R., Khan, T. A., Thounthong, P., Analytic approximate solutions for some nonlinear Parabolic dynamical wave equations, *Journal of Taibah University for Science* 14 (2020) 346-358.
- [16] Ahmad, H., Seadawy, A. R., Khan, T. A., Study on numerical solution of dispersive water wave phenomena by using a reliable modification of variational iteration algorithm, *Mathematics and Computers in Simulation* (2020) doi: 10.1016/j.matcom.2020.04.005.
- [17] Ahmad, H., Seadawy, A. R., Khan, T. A., Thounthong, P., Analytic approximate solutions for some nonlinear Parabolic dynamical wave equations, *Journal of Taibah University for Science* 14 (2020) 346-358.
- [18] Ghazanfari, S. A., Wahid, M. A., Heat transfer enhancement and pressure drop for fin-and-tube compact heat exchangers with delta winglet-type vortex generators, *Facta Universitatis, Series: Mechanical Engineering* 16 (2) (2018) 233-247.
- [19] Ahmad, H., Khan, T. A., Durur, H., Ismail, G. M. & Yokus, A., Analytic approximate solutions of diffusion equations arising in oil pollution, *Journal of Ocean Engineering and Science*, 2020, doi: <https://doi.org/10.1016/j.joes.2020.05.002>.
- [20] Ahmad, H., Khan, T. A. & Yao, S. W., An efficient approach for the numerical solution of fifth-order KdV equations, *Open Mathematics*, 18, 2020, 738-748.
- [21] Siraj-ul-Islam, Ahmad I., A comparative analysis of local meshless formulation for multi-asset option models, *Engineering Analysis with Boundary Elements* 65 (2016) 159-176.
- [22] Ahmad I, Ahmad H, Thounthong P, Chu YM, Cesarano C. Solution of Multi-Term Time-Fractional PDE Models Arising in Mathematical Biology and Physics by Local Meshless Method, *Symmetry*, 12(7), 2020, 1195.
- [23] Ahmad I., Ahsan M., Zaheer-ud-Din, Ahmad M., Kumam P., An efficient local formulation for time-dependent PDEs, *Mathematics* 7 (2019) 216.



**ORCID iD**Imtiaz Ahmad  <https://orcid.org/0000-0002-4023-3293>Hijaz Ahmad  <https://orcid.org/0000-0002-5438-5407>

© 2020 by the authors. Licensee SCU, Ahvaz, Iran. This article is an open access article distributed under the terms and conditions of the Creative Commons Attribution-NonCommercial 4.0 International (CC BY-NC 4.0 license) (<http://creativecommons.org/licenses/by-nc/4.0/>).

How to cite this article: Khan M.N., Ahmad I., Ahmad H. A Radial Basis Function Collocation Method for Space-dependent Inverse Heat Problems, *J. Appl. Comput. Mech.*, 6(SI), 2020, 1187–1199. <https://doi.org/10.22055/JACM.2020.32999.2123>

